
Since January 2020 Elsevier has created a COVID-19 resource centre with free information in English and Mandarin on the novel coronavirus COVID-19. The COVID-19 resource centre is hosted on Elsevier Connect, the company's public news and information website.

Elsevier hereby grants permission to make all its COVID-19-related research that is available on the COVID-19 resource centre - including this research content - immediately available in PubMed Central and other publicly funded repositories, such as the WHO COVID database with rights for unrestricted research re-use and analyses in any form or by any means with acknowledgement of the original source. These permissions are granted for free by Elsevier for as long as the COVID-19 resource centre remains active.

Virology 399 (2010) 120–128

Contents lists available at ScienceDirect

Virology

journal homepage: www.elsevier.com/locate/yviro

# Immunization with an attenuated severe acute respiratory syndrome coronavirus deleted in E protein protects against lethal respiratory disease

Jason Netland [a], Marta L. DeDiego [b], Jincun Zhao [c], Craig Fett [c], Enrique Álvarez [b], José L. Nieto-Torres [b], Luis Enjuanes [b], Stanley Perlman [a,c,*]

[a] Interdisciplinary Program in Immunology, University of Iowa, Iowa City, IA 52242
[b] Department of Molecular and Cell Biology, Centro Nacional de Biotecnolgia (CSIC), Campus Universidad Autonoma, Darwin 3, Cantoblanco, 28049 Madrid, Spain
[c] Department of Microbiology, University of Iowa, Iowa City, IA 52242

ARTICLE INFO

*Article history:*
Received 4 November 2009
Returned to author for revision
19 December 2009
Accepted 5 January 2010
Available online 27 January 2010

*Keywords:*
Severe acute respiratory syndrome
Rodent model
Vaccine
Coronavirus
Respiratory virus
T cell response

ABSTRACT

The severe acute respiratory syndrome coronavirus (SARS-CoV) caused substantial morbidity and mortality in 2002–2003. Deletion of the envelope (E) protein modestly diminished virus growth in tissue culture but abrogated virulence in animals. Here, we show that immunization with rSARS-CoV-ΔE or SARS-CoV-Δ[E,6-9b] (deleted in accessory proteins (6, 7a, 7b, 8a, 8b, 9b) in addition to E) nearly completely protected BALB/c mice from fatal respiratory disease caused by mouse-adapted SARS-CoV and partly protected hACE2 Tg mice from lethal disease. hACE2 Tg mice, which express the human SARS-CoV receptor, are extremely susceptible to infection. We also show that rSARS-CoV-ΔE and rSARS-CoV-Δ[E,6-9b] induced anti-virus T cell and antibody responses. Further, the E-deleted viruses were stable after 16 blind passages through tissue culture cells, with only a single mutation in the surface glycoprotein detected. The passaged virus remained avirulent in mice. These results suggest that rSARS-CoV-ΔE is an efficacious vaccine candidate that might be useful if SARS recurred.

© 2010 Elsevier Inc. All rights reserved.

## Introduction

The severe acute respiratory syndrome, caused by a novel coronavirus (SARS-CoV), infected 8000 individuals in 2002–2003, with an approximate 10% mortality rate (Peiris et al., 2004). The disease has not recurred to a significant extent since 2003, but coronaviruses similar to the one that caused the epidemic continue to circulate in wild animals, especially in bat populations (Woo et al., 2006). The SARS epidemic sparked efforts to develop vaccines that would be used if future outbreaks of SARS occurred. Both inactivated and live, attenuated vaccines have been described but thus far all are in early stages of development. From these initial studies, several salient observations emerged. First, transfer of neutralizing antibody, directed against the surface (S) glycoprotein, prior to infection completely protected experimentally infected animals from clinical disease (Greenough et al., 2005; Rockx et al., 2008; Subbarao et al., 2004; Zhu et al., 2007). Second, SARS-CoV vaccines were more effective in young than aged animal populations in terms of protection from clinical disease and the development of a neutralizing antibody response (Deming et al., 2006). Third, the precise viral proteins that were included in a particular vaccine was an important consideration because vaccines that included the nucleocapsid (N) protein resulted in an immunopathological pulmonary disease characterized by eosinophilic infiltration in SARS-CoV-challenged mice (Deming et al., 2006; Yasui et al., 2008).

In general, live attenuated vaccines offer the most protection against subsequent challenge with virulent virus because they induce both humoral and T-cell-mediated immune responses. Live, attenuated coronavirus vaccines have been developed against coronavirus pathogens such as infectious bronchitis virus and transmissible gastroenteritis virus (Saif, 2004). An additional issue that must be considered in developing a SARS-CoV vaccine is that the virus most likely originated from a SARS-like CoV that infected bats (Lau et al., 2005; Li et al., 2005). This virus then jumped species to infect intermediate hosts such as Himalayan palm civets in wet markets in Southern China prior to infecting humans (Chinese, 2004). Therefore, an ideal vaccine will also have efficacy against zoonotic strains of SARS-CoV, thereby minimizing the likelihood that virus will have sufficient time to adapt to human populations.

SARS-CoV, like other coronaviruses, is an RNA virus that replicates in the cytoplasm. The virion envelope contains at least three structural proteins, S, E and M, embedded in the membrane. Also like other coronaviruses, SARS-CoV encodes several group-specific proteins, termed 3a, 3b, 6, 7a, 7b, 8 and 9b (Snijder et al., 2003). These proteins are not essential for replication in tissue culture cells and their deletion does not significantly attenuate virus growth in mice

* Corresponding author. Department of Microbiology, BSB 3-712, University of Iowa, Iowa City, IA 52242, USA. Fax: 319 335 9999.
*E-mail address:* Stanley-Perlman@uiowa.edu (S. Perlman).

0042-6822/$ – see front matter © 2010 Elsevier Inc. All rights reserved.
doi:10.1016/j.virol.2010.01.004

(DeDiego et al., 2008; Yount et al., 2005). By contrast, deletion of the small envelope (E) protein modestly reduces SARS-CoV growth *in vitro* and *in vivo* (DeDiego et al., 2007, 2008), resulting in an attenuated virus. In other coronaviruses, deletion of E results in either complete absence of infectious virus or a severe reduction in titer (Kuo and Masters, 2003; Ortego et al., 2007). However, E deletion in the context of SARS-CoV results in only a 20-fold decrease in virus titer in tissue culture cells (DeDiego et al., 2007).

While SARS-CoV infects and replicates in several species, including mice, ferrets, hamsters and non-human primates, most of these animals develop inapparent or mild disease (reviewed in Subbarao and Roberts, 2006). Mice that are transgenic (Tg) for the expression of the human SARS-CoV receptor, angiotensin-converting enzyme 2 (hACE2) have been obtained (McCray et al., 2006; Tseng et al., 2006). These mice develop moderate respiratory disease but overwhelming neurological disease with 100% mortality after intranasal infection with SARS-CoV. As such, they are very useful to assess vaccine safety and efficacy. We previously showed that infection of these highly susceptible mice with recombinant SARS-CoV deleted in E (rSARS-CoV-ΔE) or E and several group-specific proteins genes (6, 7a, 7b, 8a, 8b and 9b; rSARS-CoV-[ΔE,6-9b]) resulted in no weight loss or death, even after inoculation with 12,000 plaque forming units (PFU). In contrast, 100% of mice infected with 800 PFU of either rSARS-CoV or rSARS-CoV deleted in group-specific genes 6, 7a, 7b, 8a, 8b and 9b (rSARS-CoV-[Δ6-9b]) succumbed to the infection (DeDiego et al., 2008). While these results suggest that rSARS-CoV-ΔE and rSARS-CoV-Δ[E,6-9b] have the potential to be safe vaccines, their stability, efficacy and immunogenicity were not examined in this initial study.

Additionally, rSARS-CoV-ΔE and rSARS-CoV-Δ[E,6-9b] were not evaluated in the context of a severe pulmonary infection, the most important manifestation of disease in infected humans. The recent isolation of SARS-CoV adapted to growth in mice or rats (Nagata et al., 2007, 2008; Roberts et al., 2007) provides a useful system for vaccine evaluation because some strains of mice and rats infected with these viruses develop severe respiratory disease. In specific, the MA15 strain was isolated after 15 passages through the lungs of BALB/c mice and unlike the parental Urbani strain of virus, intranasal inoculation with this virus results in signs of respiratory disease with substantial mortality (Roberts et al., 2007). Here, we use this infection system to assess the protective ability of rSARS-CoV-ΔE and rSARS-CoV-Δ[E,6-9b] in the context of respiratory disease. We also determined the antibody and T cell responses in BALB/c and hACE2 Tg mice after infection with rSARS-CoV-ΔE or rSARS-CoV-Δ[E,6-9b].

## Results

### *rSARS-CoV-ΔE or rSARS-CoV-Δ[E,6-9b] immunization protects mice against MA15-mediated respiratory disease in BALB/c mice*

Intranasal inoculation of BALB/c mice with MA15 virus resulted in clinically evident respiratory disease, with a dosage of approximately $3\times10^4$ PFU resulting in a 50% mortality rate (Roberts et al., 2007; Zhao et al., 2009). We used a challenge dosage of $1\times10^5$ PFU, which caused >70% mortality and substantial weight loss (Figs. 1C and D, triangles) in the experiments described below. We next showed that infection with 12,000 PFU of rSARS-CoV-ΔE or rSARS-CoV-Δ[E,6-9b] caused no weight loss or mortality in BALB/c mice (Figs. 1A and B). This was expected because the same dosage of virus caused no disease in hACE2 Tg mice, which are extremely susceptible to infection with the Urbani strain of SARS-CoV. To assess the protective ability of these viruses against infection with MA15 virus, 6- to 8-week-old BALB/c mice were immunized with 12,000 PFU rSARS-CoV-ΔE or rSARS-CoV-Δ[E,6-9b] and challenged 21 days later with $1\times10^5$ PFU MA15 virus (Figs. 1C and D). Following challenge, mice immunized with the deletion mutants exhibited weight loss on days 1–3 p.i., but 10/10 of rSARS-CoV-ΔE and 9/10 of rSARS-CoV-Δ[E,6-9b]-immunized mice recovered and survived. In contrast, naïve mice challenged with the same dose of MA15 virus lost significantly more weight and most mice succumbed to infection at days 4–8 p.i.

To determine the effect of immunization on virus growth, titers in the lungs of naïve and immunized mice were measured at 3 and 5 days post-challenge. Immunization with rSARS-CoV-ΔE resulted in

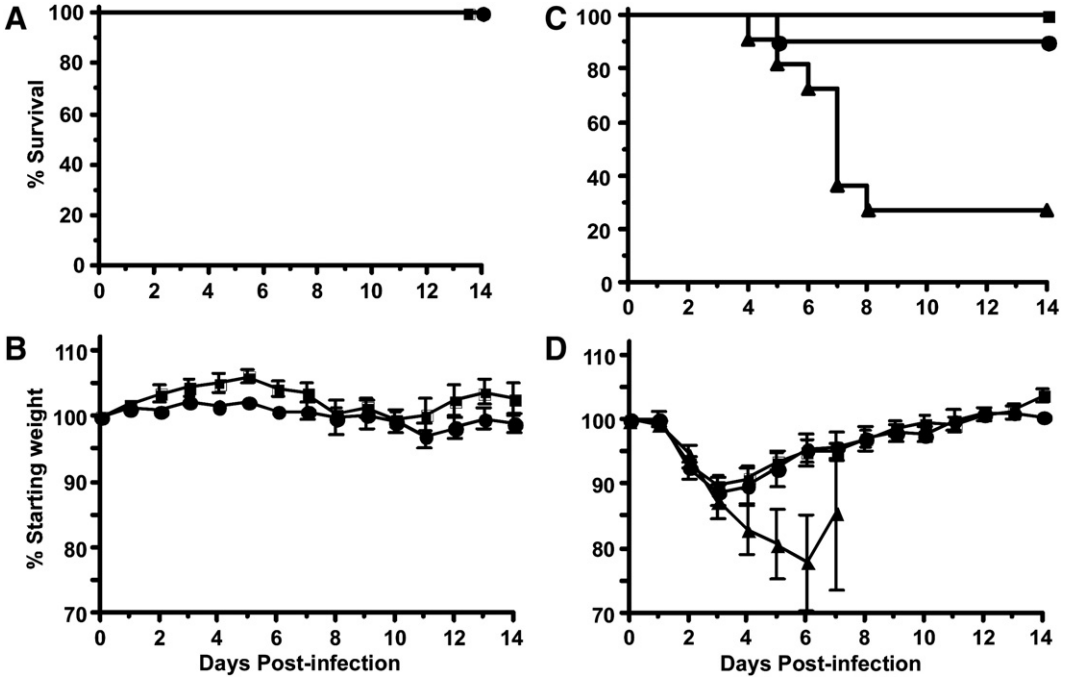


**Fig. 1.** Clinical effects and vaccine efficacy of rSARS-CoV-ΔE and rSARS-CoV-Δ[E,6-9b]. (A, B). Six-week-old BALB/c mice were infected with 12,000 PFU of rSARS-CoV-ΔE (circles, $n=10$) or rSARS-CoV-Δ[E,6-9b] (squares, $n=10$) and monitored daily for survival (A) and weight loss (B). (C, D). Six-week-old BALB/c mice were immunized with 12,000 PFU of rSARS-CoV-ΔE (circles, $n=10$) or rSARS-CoV-Δ[E,6-9b] (squares, $n=10$) or phosphate-buffered saline (PBS) (triangles, $n=11$) and challenged at day 21 post-infection with $1\times10^5$ PFU of MA15 virus. Survival (C) and weight loss (D) were recorded daily. Differences in survival were statistically significant ($p<0.002$).

8% and 91% reductions in virus titers in the lungs at days 3 and 5 p.i., respectively (Fig. 2A). MA15 virus caused pathological changes consistent with pneumonia, including alveolar edema, alveolar sloughing, necrotizing bronchiolitis and interstitial and perivascular inflammatory cell infiltration (Roberts et al., 2007; Figs. 2D and E). Vaccination with rSARS-CoV-ΔE resulted in a substantial diminution in the extent of pathological changes in challenged mice, with little evidence of lung destruction or inflammatory cell infiltration present (Figs. 2B and C). These results showed that a single dose of rSARS-CoV-ΔE was able to protect mice from clinical disease, prevent lung damage and decrease virus replication.

*Immunization is partially protective in hACE2 Tg mice challenged with the Urbani strain*

As described above, hACE2 Tg mice are exquisitely sensitive to infection with wild-type SARS-CoV with an $LD_{50}$ of approximately 240 PFU (DeDiego et al., 2008; McCray et al., 2006). Severe disease occurred when virus gained entry into the brain via the olfactory nerve. An effective immune response would likely need to prevent the entry of nearly all virus into brain, since once in the brain, virus spread is rapid and widespread (Netland et al., 2008). Next, we examined the protection mediated by immunization with rSARS-CoV-ΔE or rSARS-CoV-Δ[E,6-9b] after challenge with 12,000 PFU of the Urbani strain. A single immunization with either rSARS-CoV-ΔE or rSARS-CoV-Δ[E,6-9b] protected approximately 30% of mice from death after challenge with 12,000 PFU of the Urbani strain of SARS-CoV (Fig. 3). To assess whether virus titers in the brain correlated with protection, we analyzed four additional animals, one of which was asymptomatic.

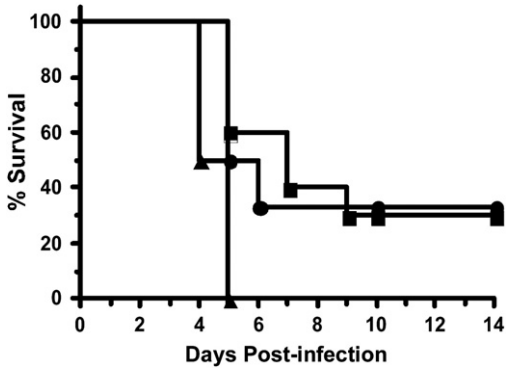


**Fig. 3.** Vaccine efficacy in SARS-CoV-infected hACE2 Tg mice. Six-week-old hACE2 Tg mice were immunized with 12,000 PFU of either rSARS-CoV-ΔE (circles, $n=6$) or rSARS-CoV-Δ[E,6-9b] (squares, $n=10$) or PBS (triangles, $n=6$) and challenged at day 21 post-immunization with 12,000 PFU of the Urbani strain of SARS-CoV. Mice were monitored daily for survival.

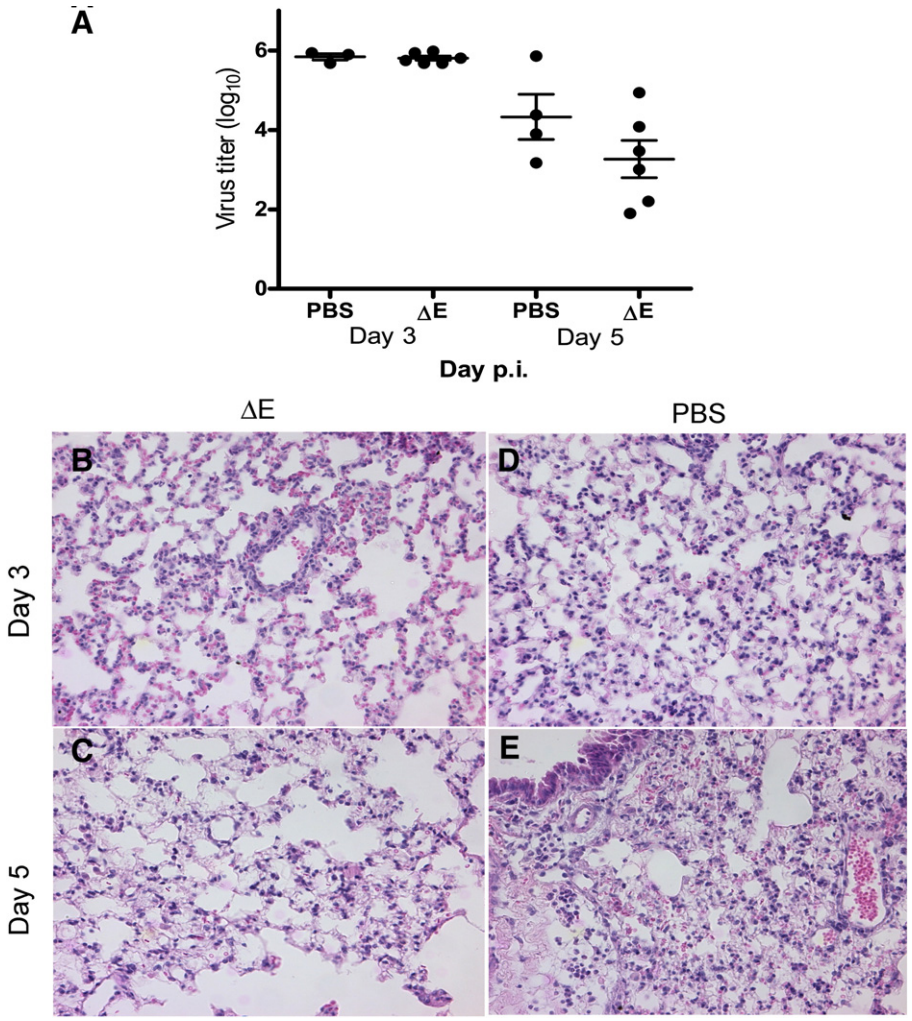


**Fig. 2.** Virus titers and pulmonary histopathological changes in MA15 virus-infected mice. Six-week-old BALB/c mice were immunized with 12,000 PFU of rSARS-CoV-ΔE or PBS and challenged at day 21 p.i. with $1\times10^5$ PFU of MA15 virus. Mice were sacrificed at days 3 and 5 post-challenge and analyzed for infectious virus (A) and histopathology (B–E) as described in Materials and Methods.

**Table 1**
Anti-SARS-CoV antibody titers measured by ELISA.

| Mouse | Virus | No. mice analyzed | Titer ± SEM |
|---|---|---|---|
| BALB/c | rSARS-CoV-ΔE | 4 | 293 ± 21 |
| | rSARS-CoV-Δ[E,6-9b] | 4 | 304 ± 34 |
| hACE2 Tg | rSARS-CoV-ΔE | 3 | 4687 ± 464 |
| | rSARS-CoV-Δ[E, 6-9b] | 3 | 3421 ± 536 |

Virus was detected in the brains of the 3 symptomatic mice (average geometric titer 7.56 ± 0.26) but not in the brain of the fourth mice. In the same experiment, average geometric titers were 8.13 ± 0.14 in the brains of PBS-treated mice, all of which developed severe disease. It should be noted that 12,000 PFU is equivalent to approximately 50 $LD_{50}$, so that even after an overwhelming infection, the vaccine showed some efficacy.

*rSARS-CoV-ΔE and rSARS-CoV-Δ[E,6-9b] immunization induces anti-virus humoral and T cell responses*

Since rSARS-CoV-ΔE and rSARS-CoV-Δ[E,6-9b] were both completely or partly protective in MA15 virus-infected BALB/c or SARS-CoV Urbani strain-infected hACE2 Tg mice, we next sought to determine the immune correlates of protection. Previous reports showed that passive administration of neutralizing antibody directed against the S protein could prevent infection (Greenough et al., 2005; Rockx et al., 2008; Subbarao et al., 2004; Zhu et al., 2007), so we initially determined anti-SARS-CoV antibody titers by ELISA and neutralization assays at 21 days after immunization with rSARS-CoV-ΔE or rSARS-CoV-Δ[E,6-9b], just prior to challenge with MA15 or Urbani strains of SARS-CoV. By ELISA, all mice mounted a detectable antibody response against whole inactivated virus (Table 1). Responses to rSARS-CoV-ΔE and rSARS-CoV-Δ[E,6-9b] were approximately 10- to 20-fold lower in BALB/c compared to hACE2 Tg mice (pooled samples, 298 ± 19 ($n = 8$) vs. 4054 ± 426 9 ($n = 6$), $p < 0.0001$). Antibody titers were higher in hACE2 Tg mice immunized with rSARS-CoV-ΔE when compared to rSARS-CoV-Δ[E,6-9b]-immunized animal, although these differences did not reach statistical significance ($p = 0.16$). Neutralizing antibody titers in the sera of the rSARS-CoV-ΔE and rSARS-CoV-Δ[E,6-9b]-immunized BALB/c mice were measured. Neutralizing antibodies were detected in all eight mice, but at low titers (titers of ≤1:10). We also measured neutralizing titers using sera from a separate group of hACE2 Tg mice immunized with rSARS-CoV-ΔE (4 mice) or rSARS-CoV-Δ[E,6-9b] (5 mice) and again detected only low levels of antibody in the sera (titers of ≤1:20 in 2/4 rSARS-CoV-ΔE and 1/5 rSARS-CoV-Δ[E,6-9b]-immunized mice).

While the role of SARS-CoV-specific T cells in virus clearance has not been directly demonstrated in patients, the importance of these cells in virus eradication in mice infected with another genus β coronavirus, mouse hepatitis virus (MHV), has been shown previously (Bergmann, Lane, and Stohlman, 2006). Thus, it is very likely that T cells are critical for virus clearance in infected humans or experimental animals. Therefore, we measured SARS-CoV-specific T cell responses in the blood of BALB/c or hACE2 Tg mice at 7 days after immunization with the MA15 or Urbani strains of virus, respectively, and in the spleen at 21 days p.i. by intracellular IFN-γ release assays. Several CD4 and CD8 T cell epitopes recognized in C57Bl/6 (H-$2^b$-restricted) and BALB/c (H-$2^d$-restricted) mice have been reported (Zhao et al., 2007; Zhi et al., 2005). Using lung mononuclear cells harvested from the lungs of MA15-infected BALB/c and C57Bl/6 mice,

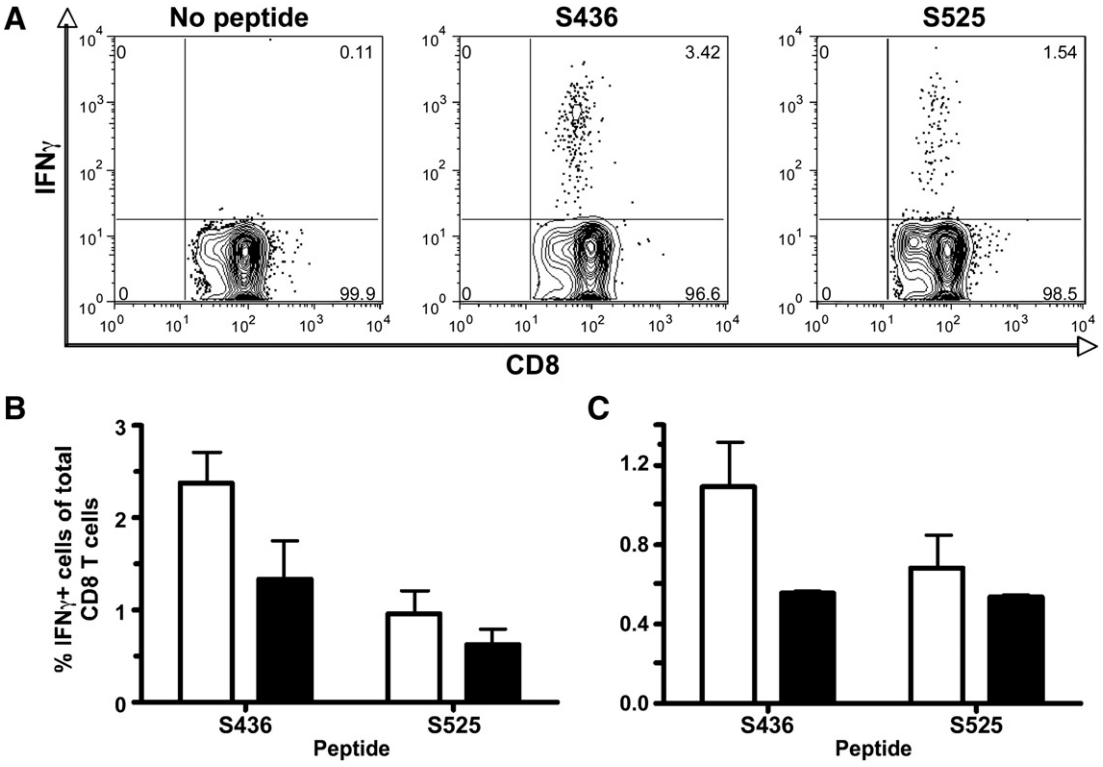


**Fig. 4.** Virus-specific CD8 T cell responses in hACE2 Tg mice after immunization with rSARS-CoV-ΔE and rSARS-CoV-Δ[E,6-9b]. Six-week-old hACE2 Tg mice were immunized by intranasal inoculation with rSARS-CoV-ΔE or rSARS-CoV-Δ[E,6-9b]. (A) Blood was obtained 7 days p.i. and the virus-specific CD8 T cell response was analyzed by intracellular IFN-γ staining as described in Materials and Methods. Representative flow cytometry plots of antigen-specific CD8 T cells in the blood of Tg mice at 7 days post-immunization with rSARS-CoV-ΔE. (B) Average frequency of S436- and S525-specific CD8 T cells in the blood of hACE2 Tg mice at day 7 post-immunization with either rSARS-CoV-ΔE (open bars, $n = 6$) or rSARS-CoV-Δ[E,6-9b] (filled bars, $n = 6$). (C) Average frequency of virus-specific CD8 T cells in the spleen of hACE2 Tg mice at day 21 post-immunization with rSARS-CoV-ΔE or rSARS-CoV-Δ[E,6-9b] ($n = 3$ for both viruses and both peptides). The number of epitope S436-specific cells were greater in the blood ($p = 0.07$) and spleen ($p = 0.08$) in rSARS-CoV-ΔE compared to rSARS-CoV-Δ[E,6-9b]-immunized mice.

we recently confirmed the identity of many of these epitopes and also identified additional epitopes (Zhao et al., 2009). We detected SARS-CoV-specific responses to seven CD8 and one CD4 T cell epitopes in the lungs of infected B6 mice, but for the purpose of assessing efficacy after immunization of hACE2 Tg mice, we measured responses in the blood to two immunodominant CD8 T cell epitopes spanning residues 436–445 and 525–534 of the surface (S) glycoprotein. Responses to both epitopes were detected in the blood of all hACE2 Tg mice at day 7 p.i. and in the spleens of mice sacrificed at day 21 p.i. (Fig. 4) with responses being higher in mice immunized with rSARS-CoV-ΔE than rSARS-CoV-Δ[E,6-9b]. Differences in responses to epitope S436 nearly reached statistical significance in the blood at day 7 (rSARS-CoV-ΔE vs. rSARS-CoV-Δ[E,6-9b], $2.4 \pm 0.3\%$, $n=6$ vs. $1.3 \pm 0.4\%$, $n=6$, $p=0.07$; Fig. 4B) and the spleen at day 21 ($1.1 \pm 0.2\%$, $n=3$, vs. $0.55 \pm 0.02\%$, $n=3$, $p=0.08$; Fig. 4C).

Three immunodominant CD8 T cell epitopes, encompassing residues 366–374, 521–529 and 1061–1071 of the spike glycoprotein and one CD4 T cell epitope (N353), were identified using lung mononuclear cells harvested from MA15 virus-infected BALB/c mice (Zhao et al., 2009). For the assays described here, we measured the CD8 T cell response to the immunodominant S366 epitope. The CD8 T cell response was less robust than detected in hACE2 Tg mice, with an S366-specific CD8 T cell response detected in the blood of 5/8 rSARS-CoV-ΔE and 7/8 rSARS-CoV-Δ[E,6-9b]-infected mice at day 7 p.i. Mean responses of those with detectable CD8 T cell responses were similar to those detected in the hACE2 Tg mice ($1.6 \pm 0.6\%$ and $1.7 \pm 0.4\%$ for rSARS-CoV-ΔE and rSARS-CoV-Δ[E,6-9b], respectively) (Fig. 5). We could not detect a SARS-CoV-specific CD8 T cell response in the spleens of immunized mice at day 21 p.i. We could not detect any CD4 T cell responses in the blood (day 7) or spleens (day 21) of immunized BALB/c mice, after cells were stimulated with peptides corresponding to epitope N353 (data not shown). Collectively, these results show that both rSARS-CoV-ΔE and rSARS-CoV-Δ[E,6-9b] induced CD8 T cells responses in BALB/c and hACE2 Tg mice.

### *A mutation in the S protein is detected after serial passage of deleted viruses in vitro*

A key feature of any live attenuated vaccine is that it must be stable after passage in tissue culture cells, or more crucially, in animals or humans. This is especially true for SARS-CoV, which rapidly underwent adaptation to replication in both intermediate hosts, such as palm civets and in human populations. SARS-CoV may have continued to adapt to human populations, if the epidemic had not been terminated so efficiently and rapidly. To address the stability of rSARS-CoV-ΔE and rSARS-CoV-Δ[E,6-9b], we serially passaged both viruses 16 times in Vero E6 cells. After passage, both viruses replicated more efficiently *in vitro*, with titers that were approximately 20-fold higher than passage 1 viruses (Fig. 6). To determine the basis of this increased ability to replicate in Vero E6 cells, we sequenced the complete genome of both passaged viruses. Remarkably, only a single mutation at position 23,312, which resulted in a serine to phenylalanine mutation, was detected in rSARS-CoV-ΔE passaged 16 times (rSARS-CoV-ΔE-p16 virus) (Table 2). This mutation, which is located outside of the receptor binding domain of the S protein, was also detected when rSARS-CoV-Δ[E, 6-9b] was passaged 16 times through Vero E6 cells (rSARS-CoV-Δ[E,6-9b]-p16). As this was the only mutation common to both viruses after tissue culture passage and the only one present in rSARS-CoV-ΔE-p16, it is likely responsible for improved replication in these cells. An additional mutation was also detected in nsp8 in rSARS-CoV-Δ[E,6-9b]-p16. The significance of this mutation, located in the primase gene, is unknown. Adaptation occurred rapidly, because the S protein mutation was detected within 5 passages through Vero E6 cells (Table 2).

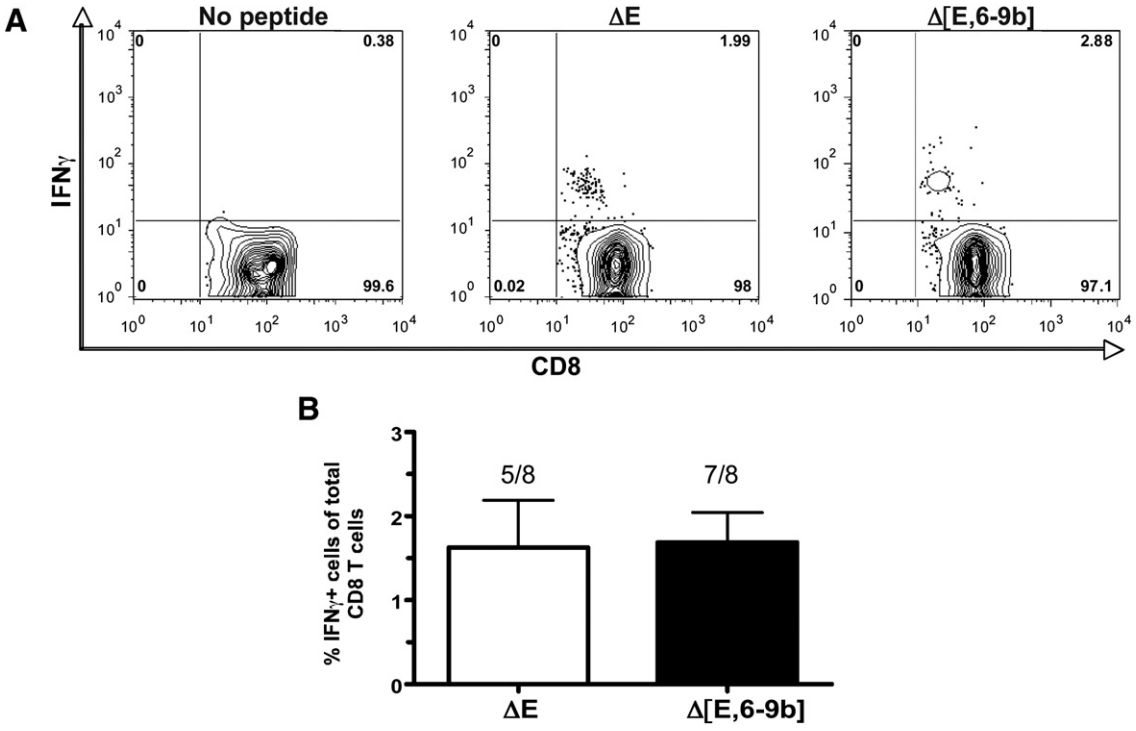


**Fig. 5.** Virus-specific CD8 T cell responses in BALB/c mice after immunization with rSARS-CoV-ΔE and rSARS-CoV-Δ[E,6-9b]. Six-week-old BALB/c mice were immunized by intranasal inoculation with rSARS-CoV-ΔE or rSARS-CoV-Δ[E,6-9b]. Blood was obtained 7 days later and the virus-specific CD8 T cell response was analyzed by intracellular IFN-γ staining. (A) Representative flow cytometry plots of antigen-specific CD8 T cells in the blood of rSARS-CoV-ΔE or rSARS-CoV-Δ[E,6-9b]-immunized BALB/c mice at 7 days post-immunization. (B) Average frequency of S366-specific CD8 T cells in the blood of BALB/c mice at day 7 post-immunization with either rSARS-CoV-ΔE (open bars) or rSARS-CoV-Δ[E,6-9b] (filled bars) ($n=8$ for both viruses ). Numbers indicate fraction of mice with detectable virus-specific CD8 T cell responses. Samples with undetectable responses were not included in the figure.

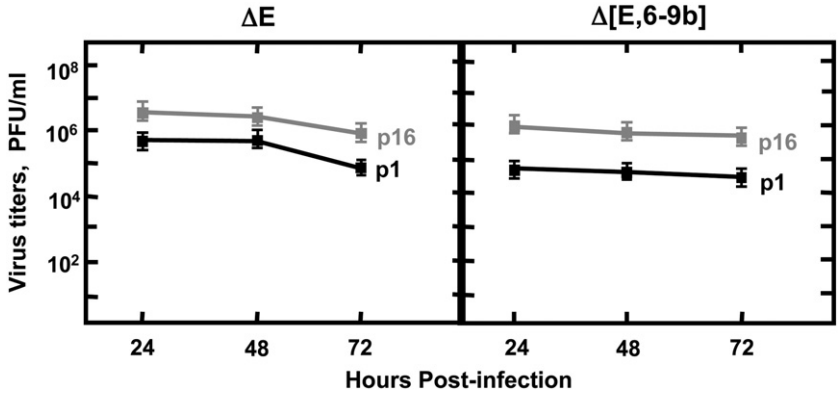


**Fig. 6.** Enhanced replication of rSARS-CoV-ΔE and rSARS-CoV-Δ(E,6-9b) after serial passage in Vero E6 cells. rSARS-CoV-ΔE and rSARS-CoV-Δ[E,6-9b] were serially passaged 16 times in Vero E6 cells. Virus was harvested and analyzed in one step growth curves by infecting Vero cells at a multiplicity of infection of 0.05. Titers were measured at the indicated times p. i. p1 and p16 indicate the original virus stock and virus passaged 16 times, respectively. Differences in titers at each time point were statistically significant ($p<0.04$).

*Increased protective ability of rSARS-CoV-ΔE-p16 against challenge with virulent virus*

To determine if rSARS-CoV-ΔE p16 and rSARS-CoV-Δ[E,6-9b] p16 were still attenuated *in vivo*, we inoculated hACE2 Tg mice with 12,000 PFU of each virus. Both rSARS-CoV-ΔE-p16 and rSARS-CoV-Δ[E,6-9b]-p16 remained attenuated with minimal mortality (1/14 and 0/18, respectively) and weight loss (Figs. 7A and B). Since both viruses grew to higher titers in tissue culture cells, we next determined if their ability to protect hACE2 Tg mice from challenge with wild-type virus was altered by passage. Immunized hACE2 Tg mice were challenged with intranasal inoculation of 12,000 PFU of the Urbani strain of SARS-CoV. rSARS-CoV-ΔE-p16 protected 60–70% of mice while rSARS-CoV-Δ[E,6-9b]-p16 protected 20–30%, suggesting that tissue culture passage did not diminish immunogenicity and, in fact, that rSARS-CoV-ΔE-p16 may mediate increased protection (Figs. 7C and D).

## Discussion

Here, we show that two attenuated viruses, rSARS-CoV-ΔE and rSARS-CoV-Δ[E,6-9b], serve as effective vaccines in preventing SARS-CoV-induced respiratory disease (Fig. 1). rSARS-CoV-Δ[E,6-9b] may ultimately be a more useful vaccine candidate because the absence of group-specific proteins 6-9b, in addition to E, makes it less likely that wild-type virus will be regenerated by recombination. Although rSARS-CoV-ΔE and rSARS-CoV-Δ[E,6-9b] were equally attenuated in our initial study (DeDiego et al., 2008), it was not expected that they would be equivalently immunogenic. Group-specific proteins have roles in inhibiting type 1 IFN signaling (ORFs 6 and 3b) and in apoptosis induction (ORF3a, ORF3b, E, M, ORF 7a, ORF 8a) (Chen et al., 2007; Frieman et al., 2007; Khan et al., 2006; Kopecky-Bromberg et al., 2006; Lai et al., 2006; Law et al., 2005; Schaecher, Mackenzie, and Pekosz, 2007; Tan et al., 2007; Yang et al., 2005; Ye et al., 2008). Therefore, deletion of these proteins might be predicted to modulate immunogenicity. This did not occur to a significant extent, although rSARS-CoV-ΔE may induce slightly higher humoral and T cell responses.

**Table 2**
Mutations identified after passage in Vero E6 tissue culture cells.

| Virus | Mutations[a] | Protein | Passage 5 | Passage 10 | Passage 16 |
|---|---|---|---|---|---|
| rSARS-CoV-ΔE | 23,312 (S-F) | S | Yes | Yes | Yes |
| rSARS-CoV-Δ[E,6-9b] | 12,287 (T-I) | Nsp8 | No | No | Yes |
| | 23,312 (S-F) | S | No | No | Yes |

[a] Mutations identified in passage 16 virus.

SARS-CoV-specific T cell and antibody responses were detected in vaccinated hACE2 Tg and BALB/c mice (Figs. 4 and 5). At present, the precise role of each response in virus clearance in patients with SARS is not well defined. Patients who recover mount good virus-specific antibody responses whereas those that develop more severe disease do not (Cameron et al., 2007). Based on studies of other coronavirus infections, it is likely that both virus-specific T cell and antibody responses are critical for virus clearance. In mice infected with MHV, CD4 and CD8 T cell responses are necessary for virus clearance during the acute phase of the infection whereas anti-MHV antibody is necessary to prevent virus recrudescence (Bergmann, Lane, and Stohlman, 2006).

Passive administration of neutralizing antibody prior to SARS-CoV infection completely prevents disease in hamsters and in wild-type and hACE2 Tg mice (Greenough et al., 2005; McCray et al., 2006; Roberts et al., 2006; Rockx et al., 2008; Subbarao et al., 2004; Zhu et al., 2007). Immunization with rSARS-CoV-ΔE or rSARS-CoV-Δ[E,6-9b] resulted in an anti-viral antibody response, as measured by ELISA at day 21 p.i. (Table 1) although neutralizing antibody titers were low. Consistent with these results, virus-specific antibody titers in mice infected with MHV, when measured by ELISA, reached a maximum at about 20 days p.i. while neutralizing titers were detectable at 10 days p.i. but did not reach peak values until 45 days p.i. (Tschen et al., 2006). Future goals will be to determine whether the kinetics of the development of neutralizing antibodies follows the same pattern as that of MHV and whether protection is long lasting.

Our results also showed that tissue culture adaptation resulted in a virus that was more immunogenic. One hACE2 Tg mouse died after infection with rSARS-CoV-ΔE p16, but a greater percentage of mice challenged with rSARS-CoV survived when compared to those immunized with unpassaged virus (Figs. 1 and 7). It should be noted that the gain in virulence was relatively minor since the $LD_{50}$ of SARS-CoV in hACE2 Tg mice is 250–800 PFU while only 1/20 hACE2 Tg mice died after infection with 12,000 PFU rSARS-CoV-ΔE p16. No evidence for increased virulence was observed in BALB/c mice, consistent with the extreme susceptibility to infection exhibited by hACE2 Tg mice. Tissue culture adaptation of viruses most often results in the generation of viruses that are attenuated in animals. However, SARS-CoV was in a state of active adaptation to both palm civets, an intermediate host, and humans, when the epidemic was terminated in 2003 (Chinese, 2004; Kan et al., 2005; Song et al., 2005). Thus, it may not be surprising that the virus underwent further adaptation after tissue culture cell passage. The single mutation that was detected in rSARS-CoV-ΔE was in the S protein, although not in the region responsible for binding to the host cell receptor (Wong et al., 2004). Further development of a rSARS-CoV-ΔE vaccine will require additional passage through Vero E6 and human tissue culture cells

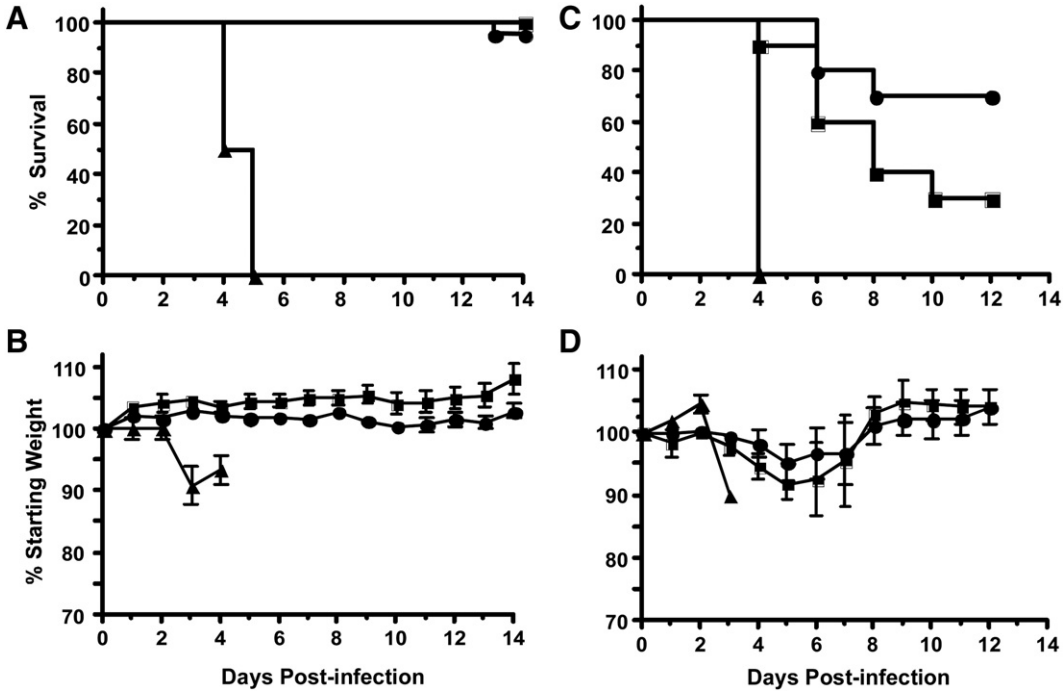


**Fig. 7.** Clinical effects and vaccine efficacy of rSARS-CoV-ΔE and rSARS-CoV-Δ[E,6-9b] after 16 passages through Vero E6 cells. (A, B). Six-week-old hACE2 Tg mice were inoculated with 12,000 PFU of rSARS-CoV-ΔE-p16 (circles, $n=14$) or rSARS-CoV-Δ[E,6-9b]-p16 (squares, $n=18$) or wild-type rSARS-CoV (triangles, $n=4$) and monitored daily for survival (A) and weight loss (B). Differences in survival were statistically significant ($p<0.002$). (C, D). Six-week-old hACE2 Tg mice were immunized with 12,000 PFU of rSARS-CoV-ΔE-p16 (circles, $n=8$) or rSARS-CoV-Δ(E,6-9b)-p16 (squares, $n=10$) or PBS (triangles, $n=4$) and challenged 21 days post-immunization with 12,000 PFU of SARS-CoV Urbani. Survival (C) and weight loss (D) were recorded daily.

to determine if the virus continues to undergo further adaptation to primate cells and possibly, gains (or losses) in virulence and immunogenicity. This potential for a gain in virulence indicates that it will be important to introduce additional mutations into the virus to ensure safety. One obvious candidate for mutation is nsp1, since this protein is involved in modulating the host immune response (Kamitani et al., 2006; Narayanan et al., 2008; Zust et al., 2007). Mutation of nsp1 in MHV has been shown to attenuate the virus without affecting immunogenicity, and based on the similarity between SARS-CoV and MHV nsp1 s, mutation of nsp1 is predicted to have a similar effect.

In the SARS epidemic in 2002–2003, aged populations were most at risk for developing severe disease (Peiris, Guan, and Yuen, 2004). Aged mice, like humans >60 years of age, are more susceptible to SARS-CoV and do not mount effective immune responses to SARS-CoV immunogens that are effective in younger populations (Deming et al., 2006). It will be important to determine if rSARS-CoV-ΔE and rSARS-CoV-Δ[E,6-9b] are both safe and efficacious in these populations.

Collectively, the data described above suggest that rSARS-CoV-ΔE and rSARS-CoV-Δ[E,6-9b] are useful vaccine candidates. These vaccines are safe, protect against challenge with SARS-CoV in two rodent infections and induce T cell and antibody responses. Further, no evidence of immunopathological disease in the BALB/c lung was detected after immunization with either virus and challenge with virulent virus.

## Materials and methods

### *Animals*

Human angiotensin-converting enzyme 2 transgenic mice (K18-hACE2, H-2$^b$-restricted) were generated as previously described (McCray et al., 2006). Pathogen-free BALB/c mice were purchased from the National Cancer Institute. All animal studies were approved by the University of Iowa Animal Care and Use Committee.

### *Viruses and cells*

SARS-CoV (Urbani strain) was obtained from W. Bellini and T. Ksiazek at the Centers for Disease Control, Atlanta, GA. The mouse-adapted MA15 strain of SARS-CoV (MA15) was generously provided by K. Subbarao (NIH). Recombinant strains of SARS-CoV (rSARS-CoV, rSARS-CoV-ΔE and rSARS-CoV-Δ[E,6-9b]) were generated as previously described (DeDiego et al., 2007, 2008). Virus was propagated and titers determined on Vero E6 cells (ATCC, Manassas, VA).

### *Mouse infections*

Mice were lightly anesthetized with isoflurane and virus was administered intranasally in 30 μl of Dulbecco's modified Eagle's medium. Mice were immunized intranasally with $1.2\times10^4$ PFU of recombinant viruses (unpassaged or passaged). In challenge experiments, hACE2 Tg mice were inoculated with $1.2\times10^4$ PFU of wild-type SARS-CoV, and BALB/c mice were inoculated with $1\times10^5$ PFU of MA15 intranasally. All SARS-CoV work was performed in the University of Iowa BSL3 Laboratory Core Facility.

### *Histopathological examination of lungs of infected mice*

Animals were anaesthetized and transcardially profused with phosphate-buffered saline followed by zinc formalin. Lungs were inflated with zinc formalin, removed and fixed overnight in zinc formalin before being paraffin embedded, sectioned and stained with hematoxylin and eosin.

### *Measurement of ELISA titers*

Whole blood was collected from immunized mice at 21 days post-infection and sera were prepared. ELISA titers were performed as follows. The 96-well Maxisorp Immuno Plates (Nunc) were coated with $2\times10^5$ PFU of formaldehyde and UV-inactivated SARS-CoV (BEI

Resources, Manassas, VA). After washing, wells were exposed to threefold dilutions of sera from naïve or immunized mice for 1.5 h. Wells were washed and then treated sequentially with 1:2000 dilution of peroxidase-conjugated Protein A (Bio-Rad, Hercules, CA) for 1 h at 37 °C and tetramethylbenzidine (K-Blue MAX TMB substrate, Neogen Corporation, Lexington, KY) for 10 min at room temperature. Reactions were stopped with 1.5 M $H_2SO_4$, and the absorbance was read at 450 nm. The ELISA titer was defined as the highest dilution of the serum giving a twofold increase over the background.

*Measurement of neutralizing antibody titers*

A virus plaque reduction assay was used to determine serum neutralizing antibody titers. Sera were diluted at the indicated ratios and incubated with 50 PFU of SARS-CoV for 30 min. Plaque assays were performed as previously described (DeDiego et al., 2007).

*Measurement of CD8 and CD4 T cell responses*

Virus-specific CD8 and CD4 T cells were measured by intracellular cytokine staining (ICS) for IFN-γ after a 5-h incubation in brefeldin A (BD Pharmingen, San Diego, CA) in the presence or absence of SARS-CoV peptides. For hACE2 Tg mice (H-$2^b$-restricted), peptides corresponding to two previously identified CD8 T cell epitopes encompassing residues 436–443 (S436) and 525–532 (S525) of the S protein were used (Zhi et al., 2005). For BALB/c mice, peptides corresponding to a previously identified CD8 T cell epitope encompassing residues 366–374 of the S protein (S366) and a CD4 T cell epitope contained in residues 353–370 of the N protein (N353) were used (Zhao et al., 2007; Zhi et al., 2005). To measure T cell responses in the blood, CHB3 (S436 and S525), P815 (S366) or A20 (N353) cells were coated with 1 μM of peptide prior to the 5-h brefeldin A incubation. Cells were stained with fluorescein isothiocyanate (FITC)-conjugated anti-CD8 or anti CD4 mAb and allophycocyanin (APC)-conjugated anti-IFN-γ mAbs (BD Pharmingen) as described previously (Wu et al., 2000).

*Derivation and analysis of tissue culture cell-passaged virus*

To generate passaged viruses, viral stocks were initially inoculated onto confluent Vero E6 cells seeded in F12.5 $cm^2$ flasks. One third of viral supernatants from infected cells were serially passaged 16 times onto fresh cells at 24 h post-infection (hr p.i.). At passages 5, 10 and 16, viruses were titered. For *in vitro* growth kinetics, Vero E6 cells in F12.5 $cm^2$ flasks were inoculated with the passaged virus at a multiplicity of infection (moi) of 0.05. After absorption for 1 h, the inoculum was removed and 3 ml of fresh medium was added. Supernatants of the infected cells were titered at 24, 48 and 72 hr p.i.

*Sequencing of viral RNA*

Total RNA from infected Vero E6 cells was isolated using an RNeasy mini kit (Qiagen, Hilden, Germany) or Trizol (Invitrogen, Carlsbad, CA). Two micrograms of RNA was reverse transcribed as previously described (Pewe et al., 1996). A series of overlapping PCR products that covered the entire SARS-CoV genome were generated using Amplitaq polymerase (Applied Biosystems). PCR products were sequenced using the forward and reverse primers used to generate the products and an Applied Biosystems Model 3730 DNA Sequencer. All mutations were confirmed using at least two independently derived samples of infected cell RNA.

*Statistical analysis*

A Student's *t* test was used to analyze differences in mean values between groups. All results are expressed as means ± standard errors of the means (SEM). $p$ values of $<0.05$ were considered statistically significant.

## Acknowledgments

This work was supported by grants from the National Institutes of Health (US) (PO1 AI060699-01) (SP); RO1 AI079424-01A1 (SP and LE), the Ministry of Education and Science of Spain (BIO2007-60978) (LE) and the European Commission (EMPERIE PROJECT, Ref. No. 223498) (LE). J.N. was supported by an NIH training grant (T32 AI007533).

## References

Bergmann, C.C., Lane, T.E., Stohlman, S.A., 2006. Coronavirus infection of the central nervous system: host–virus stand-off. Nat. Rev. Microbiol. 4 (2), 121–132.
Cameron, M.J., Ran, L., Xu, L., Danesh, A., Bermejo-Martin, J.F., Cameron, C.M., Muller, M.P., Gold, W.L., Richardson, S.E., Poutanen, S.M., Willey, B.M., Devries, M.E., Fang, Y., Seneviratne, C., Bosinger, S.E., Persad, D., Wilkinson, P., Greller, L.D., Somogyi, R., Humar, A., Keshavjee, S., Louie, M., Loeb, M.B., Brunton, J., McGeer, A.J., Kelvin, D.J., 2007. Interferon-mediated immunopathological events are associated with atypical innate and adaptive immune responses in patients with severe acute respiratory syndrome. J. Virol. 81 (16), 8692–8706.
Chen, C.Y., Ping, Y.H., Lee, H.C., Chen, K.H., Lee, Y.M., Chan, Y.J., Lien, T.C., Jap, T.S., Lin, C.H., Kao, L.S., Chen, Y.M., 2007. Open reading frame 8a of the human severe acute respiratory syndrome coronavirus not only promotes viral replication but also induces apoptosis. J. Infect. Dis. 196 (3), 405–415.
Chinese, S.M.E.C., 2004. Molecular evolution of the SARS coronavirus during the course of the SARS epidemic in China. Science 303 (5664), 1666–1669.
DeDiego, M.L., Alvarez, E., Almazan, F., Rejas, M.T., Lamirande, E., Roberts, A., Shieh, W.J., Zaki, S.R., Subbarao, K., Enjuanes, L., 2007. A severe acute respiratory syndrome coronavirus that lacks the E gene is attenuated in vitro and in vivo. J. Virol. 81 (4), 1701–1713.
DeDiego, M.L., Pewe, L., Alvarez, E., Rejas, M.T., Perlman, S., Enjuanes, L., 2008. Pathogenicity of severe acute respiratory coronavirus deletion mutants in hACE-2 transgenic mice. Virology 376 (2), 379–389.
Deming, D., Sheahan, T., Heise, M., Yount, B., Davis, N., Sims, A., Suthar, M., Harkema, J., Whitmore, A., Pickles, R., West, A., Donaldson, E., Curtis, K., Johnston, R., Baric, R., 2006. Vaccine efficacy in senescent mice challenged with recombinant SARS-CoV bearing epidemic and zoonotic spike variants. PLoS Med. 3 (12), e525.
Frieman, M., Yount, B., Heise, M., Kopecky-Bromberg, S.A., Palese, P., Baric, R.S., 2007. Severe acute respiratory syndrome coronavirus ORF6 antagonizes STAT1 function by sequestering nuclear import factors on the rough endoplasmic reticulum/Golgi membrane. J. Virol. 81 (18), 9812–9824.
Greenough, T.C., Babcock, G.J., Roberts, A., Hernandez, H.J., Thomas Jr., W.D., Coccia, J.A., Graziano, R.F., Srinivasan, M., Lowy, I., Finberg, R.W., Subbarao, K., Vogel, L., Somasundaran, M., Luzuriaga, K., Sullivan, J.L., Ambrosino, D.M., 2005. Development and characterization of a severe acute respiratory syndrome-associated coronavirus-neutralizing human monoclonal antibody that provides effective immunoprophylaxis in mice. J. Infect. Dis. 191 (4), 507–514.
Kamitani, W., Narayanan, K., Huang, C., Lokugamage, K., Ikegami, T., Ito, N., Kubo, H., Makino, S., 2006. Severe acute respiratory syndrome coronavirus nsp1 protein suppresses host gene expression by promoting host mRNA degradation. Proc. Natl. Acad. Sci. U.S.A. 103 (34), 12885–12890.
Kan, B., Wang, M., Jing, H., Xu, H., Jiang, X., Yan, M., Liang, W., Zheng, H., Wan, K., Liu, Q., Cui, B., Xu, Y., Zhang, E., Wang, H., Ye, J., Li, G., Li, M., Cui, Z., Qi, X., Chen, K., Du, L., Gao, K., Zhao, Y.T., Zou, X.Z., Feng, Y.J., Gao, Y.F., Hai, R., Yu, D., Guan, Y., Xu, J., 2005. Molecular evolution analysis and geographic investigation of severe acute respiratory syndrome coronavirus-like virus in palm civets at an animal market and on farms. J. Virol. 79 (18), 11892–11900.
Khan, S., Fielding, B.C., Tan, T.H., Chou, C.F., Shen, S., Lim, S.G., Hong, W., Tan, Y.J., 2006. Over-expression of severe acute respiratory syndrome coronavirus 3b protein induces both apoptosis and necrosis in Vero E6 cells. Virus Res. 122 (1-2), 20–27.
Kopecky-Bromberg, S.A., Martinez-Sobrido, L., Frieman, M., Baric, R.A., Palese, P., 2006. SARS coronavirus proteins Orf 3b, Orf 6, and nucleocapsid function as interferon antagonists. J. Virol. 81, 548–557.
Kuo, L., Masters, P.S., 2003. The small envelope protein E is not essential for murine coronavirus replication. J. Virol. 77, 4597–4608.
Lai, C.W., Chan, Z.R., Yang, D.G., Lo, W.H., Lai, Y.K., Chang, M.D., Hu, Y.C., 2006. Accelerated induction of apoptosis in insect cells by baculovirus-expressed SARS-CoV membrane protein. FEBS Lett. 580 (16), 3829–3834.
Lau, S.K., Woo, P.C., Li, K.S., Huang, Y., Tsoi, H.W., Wong, B.H., Wong, S.S., Leung, S.Y., Chan, K.H., Yuen, K.Y., 2005. Severe acute respiratory syndrome coronavirus-like virus in Chinese horseshoe bats. Proc. Natl. Acad. Sci. U.S.A. 102 (39), 14040–14045.
Law, P.T., Wong, C.H., Au, T.C., Chuck, C.P., Kong, S.K., Chan, P.K., To, K.F., Lo, A.W., Chan, J.Y., Suen, Y.K., Chan, H.Y., Fung, K.P., Waye, M.M., Sung, J.J., Lo, Y.M., Tsui, S.K., 2005. The 3a protein of severe acute respiratory syndrome-associated coronavirus induces apoptosis in Vero E6 cells. J. Gen. Virol. 86 (Pt 7), 1921–1930.
Li, W., Shi, Z., Yu, M., Ren, W., Smith, C., Epstein, J.H., Wang, H., Crameri, G., Hu, Z., Zhang, H., Zhang, J., McEachern, J., Field, H., Daszak, P., Eaton, B.T., Zhang, S., Wang, L.F., 2005. Bats are natural reservoirs of SARS-like coronaviruses. Science 310 (5748), 676–679.

McCray Jr., P.B., Pewe, L., Wohlford-Lenane, C., Hickey, M., Manzel, L., Shi, L., Netland, J., Jia, H.P., Halabi, C., Sigmund, C.D., Meyerholz, D.K., Kirby, P., Look, D.C., Perlman, S., 2006. Lethal infection in K18-hACE2 mice infected with SARS-CoV. J. Virol. 81, 813–821.

Nagata, N., Iwata, N., Hasegawa, H., Fukushi, S., Yokoyama, M., Harashima, A., Sato, Y., Saijo, M., Morikawa, S., Sata, T., 2007. Participation of both host and virus factors in induction of severe acute respiratory syndrome (SARS) in F344 rats infected with SARS coronavirus. J. Virol. 81 (4), 1848–1857.

Nagata, N., Iwata, N., Hasegawa, H., Fukushi, S., Harashima, A., Sato, Y., Saijo, M., Taguchi, F., Morikawa, S., Sata, T., 2008. Mouse-passaged severe acute respiratory syndrome-associated coronavirus leads to lethal pulmonary edema and diffuse alveolar damage in adult but not young mice. Am. J. Pathol. 172 (6), 1625–1637.

Narayanan, K., Huang, C., Lokugamage, K., Kamitani, W., Ikegami, T., Tseng, C.T., Makino, S., 2008. Severe acute respiratory syndrome coronavirus nsp1 suppresses host gene expression, including that of type I interferon, in infected cells. J. Virol. 82 (9), 4471–4479.

Netland, J., Meyerholz, D.K., Moore, S., Cassell, M., Perlman, S., 2008. Severe acute respiratory syndrome coronavirus infection causes neuronal death in the absence of encephalitis in mice transgenic for human ACE2. J. Virol. 82 (15), 7264–7275.

Ortego, J., Ceriani, J.E., Patino, C., Plana, J., Enjuanes, L., 2007. Absence of E protein arrests transmissible gastroenteritis coronavirus maturation in the secretory pathway. Virology 368 (2), 296–308.

Peiris, J.S., Guan, Y., Yuen, K.Y., 2004. Severe acute respiratory syndrome. Nat. Med. 10 (12 Suppl), S88–97.

Pewe, L., Wu, G., Barnett, E.M., Castro, R., Perlman, S., 1996. Cytotoxic T cell-resistant variants are selected in a virus-induced demyelinating disease. Immunity 5, 253–262.

Roberts, A., Thomas, W.D., Guarner, J., Lamirande, E.W., Babcock, G.J., Greenough, T.C., Vogel, L., Hayes, N., Sullivan, J.L., Zaki, S., Subbarao, K., Ambrosino, D.M., 2006. Therapy with a severe acute respiratory syndrome-associated coronavirus-neutralizing human monoclonal antibody reduces disease severity and viral burden in golden Syrian hamsters. J. Infect. Dis. 193 (5), 685–692.

Roberts, A., Deming, D., Paddock, C.D., Cheng, A., Yount, B., Vogel, L., Herman, B.D., Sheahan, T., Heise, M., Genrich, G.L., Zaki, S.R., Baric, R., Subbarao, K., 2007. A mouse-adapted SARS-Coronavirus causes disease and mortality in BALB/c mice. PLoS Pathog. 3 (1), e5.

Rockx, B., Corti, D., Donaldson, E., Sheahan, T., Stadler, K., Lanzavecchia, A., Baric, R., 2008. Structural basis for potent cross-neutralizing human monoclonal antibody protection against lethal human and zoonotic severe acute respiratory syndrome coronavirus challenge. J. Virol. 82 (7), 3220–3235.

Saif, L.J., 2004. Animal coronavirus vaccines: lessons for SARS. Dev. Biol. (Basel). 119, 129–140.

Schaecher, S.R., Mackenzie, J.M., Pekosz, A., 2007. The ORF7b protein of severe acute respiratory syndrome coronavirus (SARS-CoV) is expressed in virus-infected cells and incorporated into SARS-CoV particles. J. Virol. 81 (2), 718–731.

Snijder, E.J., Bredenbeek, P.J., Dobbe, J.C., Thiel, V., Ziebuhr, J., Poon, L.L., Guan, Y., Rozanov, M., Spaan, W.J., Gorbalenya, A.E., 2003. Unique and conserved features of genome and proteome of SARS-coronavirus, an early split-off from the coronavirus group 2 lineage. J. Mol. Biol. 331, 991–1004.

Song, H.D., Tu, C.C., Zhang, G.W., Wang, S.Y., Zheng, K., Lei, L.C., Chen, Q.X., Gao, Y.W., Zhou, H.Q., Xiang, H., Zheng, H.J., Chern, S.W., Cheng, F., Pan, C.M., Xuan, H., Chen, S.J., Luo, H.M., Zhou, D.H., Liu, Y.F., He, J.F., Qin, P.Z., Li, L.H., Ren, Y.Q., Liang, W.J., Yu, Y.D., Anderson, L., Wang, M., Xu, R.H., Wu, X.W., Zheng, H.Y., Chen, J.D., Liang, G., Gao, Y., Liao, M., Fang, L., Jiang, L.Y., Li, H., Chen, F., Di, B., He, L.J., Lin, J.Y., Tong, S., Kong, X., Du, L., Hao, P., Tang, H., Bernini, A., Yu, X.J., Spiga, O., Guo, Z.M., Pan, H.Y., He, W.Z., Manuguerra, J.C., Fontanet, A., Danchin, A., Niccolai, N., Li, Y.X., Wu, C.I., Zhao, G.P., 2005. Cross-host evolution of severe acute respiratory syndrome coronavirus in palm civet and human. Proc. Natl. Acad. Sci. U.S.A. 102 (7), 2430–2435.

Subbarao, K., McAuliffe, J., Vogel, L., Fahle, G., Fischer, S., Tatti, K., Packard, M., Shieh, W. J., Zaki, S., Murphy, B., 2004. Prior infection and passive transfer of neutralizing antibody prevent replication of severe acute respiratory syndrome coronavirus in the respiratory tract of mice. J. Virol. 78 (7), 3572–3577.

Subbarao, K., Roberts, A., 2006. Is there an ideal animal model for SARS? Trends Microbiol. 14 (7), 299–303.

Tan, Y.X., Tan, T.H., Lee, M.J., Tham, P.Y., Gunalan, V., Druce, J., Birch, C., Catton, M., Fu, N.Y., Yu, V.C., Tan, Y.J., 2007. Induction of apoptosis by the severe acute respiratory syndrome coronavirus 7a protein is dependent on its interaction with the Bcl-XL protein. J. Virol. 81 (12), 6346–6355.

Tschen, S.I., Stohlman, S.A., Ramakrishna, C., Hinton, D.R., Atkinson, R.D., Bergmann, C.C., 2006. CNS viral infection diverts homing of antibody-secreting cells from lymphoid organs to the CNS. Eur. J. Immunol. 36 (3), 603–612.

Tseng, C.T., Huang, C., Newman, P., Wang, N., Narayanan, K., Watts, D.M., Makino, S., Packard, M., Zaki, S.R., Chan, T.S., Peters, C.J., 2006. SARS coronavirus infection of mice transgenic for the human angiotensin-converting enzyme 2 (hACE2) virus receptor. J. Virol. 81, 1162–1173.

Wong, S.K., Li, W., Moore, M.J., Choe, H., Farzan, M., 2004. A 193-amino acid fragment of the SARS coronavirus S protein efficiently binds angiotensin-converting enzyme 2. J. Biol. Chem. 279 (5), 3197–3201.

Woo, P.C., Lau, S.K., Li, K.S., Poon, R.W., Wong, B.H., Tsoi, H.W., Yip, B.C., Huang, Y., Chan, K.H., Yuen, K.Y., 2006. Molecular diversity of coronaviruses in bats. Virology 351 (1), 180–187.

Wu, G.F., Dandekar, A.A., Pewe, L., Perlman, S., 2000. CD4 and CD8 T cells have redundant but not identical roles in virus-induced demyelination. J. Immunol. 165, 2278–2286.

Yang, Y., Xiong, Z., Zhang, S., Yan, Y., Nguyen, J., Ng, B., Lu, H., Brendese, J., Yang, F., Wang, H., Yang, X.F., 2005. Bcl-xL inhibits T-cell apoptosis induced by expression of SARS coronavirus E protein in the absence of growth factors. Biochem. J. 392 (Pt 1), 135–143.

Yasui, F., Kai, C., Kitabatake, M., Inoue, S., Yoneda, M., Yokochi, S., Kase, R., Sekiguchi, S., Morita, K., Hishima, T., Suzuki, H., Karamatsu, K., Yasutomi, Y., Shida, H., Kidokoro, M., Mizuno, K., Matsushima, K., Kohara, M., 2008. Prior immunization with severe acute respiratory syndrome (SARS)-associated coronavirus (SARS-CoV) nucleocapsid protein causes severe pneumonia in mice infected with SARS-CoV. J. Immunol. 181 (9), 6337–6348.

Ye, Z., Wong, C.K., Li, P., Xie, Y., 2008. A SARS-CoV protein, ORF-6, induces caspase-3 mediated, ER stress and JNK-dependent apoptosis. Biochim. Biophys. Acta 1780 (12), 1383–1387.

Yount, B., Roberts, R.S., Sims, A.C., Deming, D., Frieman, M.B., Sparks, J., Denison, M.R., Davis, N., Baric, R.S., 2005. Severe acute respiratory syndrome coronavirus group-specific open reading frames encode nonessential functions for replication in cell cultures and mice. J. Virol. 79 (23), 14909–14922.

Zhao, J., Huang, Q., Wang, W., Zhang, Y., Lv, P., Gao, X.M., 2007. Identification and characterization of dominant helper T-cell epitopes in the nucleocapsid protein of severe acute respiratory syndrome coronavirus. J. Virol. 81 (11), 6079–6088.

Zhao, J., Zhao, J., Van Rooijen, N., Perlman, S., 2009. Evasion by stealth: Inefficient immune activation underlies poor T cell response and severe disease in SARS-CoV-infected mice. PLoS Pathog. 5 (10), e1000636.

Zhi, Y., Kobinger, G.P., Jordan, H., Suchma, K., Weiss, S.R., Shen, H., Schumer, G., Gao, G., Boyer, J.L., Crystal, R.G., Wilson, J.M., 2005. Identification of murine CD8 T cell epitopes in codon-optimized SARS-associated coronavirus spike protein. Virology 335 (1), 34–45.

Zhu, Z., Chakraborti, S., He, Y., Roberts, A., Sheahan, T., Xiao, X., Hensley, L.E., Prabakaran, P., Rockx, B., Sidorov, I.A., Corti, D., Vogel, L., Feng, Y., Kim, J.O., Wang, L.F., Baric, R., Lanzavecchia, A., Curtis, K.M., Nabel, G.J., Subbarao, K., Jiang, S., Dimitrov, D.S., 2007. Potent cross-reactive neutralization of SARS coronavirus isolates by human monoclonal antibodies. Proc. Natl. Acad. Sci. U.S.A. 104 (29), 12123–12128.

Zust, R., Cervantes-Barragan, L., Kuri, T., Blakqori, G., Weber, F., Ludewig, B., Thiel, V., 2007. Coronavirus non-structural protein 1 is a major pathogenicity factor: implications for the rational design of coronavirus vaccines. PLoS Pathog. 3 (8), e109.